

Diffraction on nuclei: Effects of nucleon correlations

M. Alvioli

Davey Laboratory, Pennsylvania State University, University Park, Pennsylvania 16803, USA

C. Ciofi degli Atti

*Department of Physics, University of Perugia, Perugia, Via A. Pascoli, I-06123, Italy and
Istituto Nazionale di Fisica Nucleare, Sezione di Perugia, Perugia, Via A. Pascoli, I-06123, Italy*

B. Z. Kopeliovich, I. K. Potashnikova, and Iván Schmidt

*Departamento de Física, Centro de Estudios Subatómicos, Universidad Técnica Federico Santa María, Casilla 110-V, Valparaíso, Chile and
Centro Científico-Tecnológico de Valparaíso, Casilla 110-V, Valparaíso, Chile*

(Received 15 November 2009; published 25 February 2010)

The cross sections for a variety of diffractive processes in proton-nucleus scattering, associated with large gaps in rapidity, are calculated within an improved Glauber-Gribov theory, where the inelastic shadowing corrections are summed to all orders by employing the dipole representation. The effects of nucleon correlations, leading to a modification of the nuclear thickness function, are also taken into account. Numerical calculations are performed for the energies of the Hadron-Electron Ring Accelerator-B experiment, the Relativistic Heavy Ion Collider and Large Hadron Collider, and for several nuclei. It is found that whereas the Gribov corrections generally make nuclear matter more transparent, nucleon correlations act in the opposite direction and have important effects in various diffractive processes.

DOI: [10.1103/PhysRevC.81.025204](https://doi.org/10.1103/PhysRevC.81.025204)

PACS number(s): 24.85.+p, 13.85.Lg, 25.55.Ci

I. INTRODUCTION

In hadron-nucleus collisions at high energies, nuclei act almost like “black” absorbers. Therefore the optical analogy should be relevant, and diffraction appears to be an important process. Experimentally, diffraction appears as large-rapidity gap events, when the debris of the projectile hadron and the nucleus occupy only small rapidity intervals close to the rapidities of the colliding particles. The optical analogy is employed by the Glauber theory [1] of hadron-nucleus interactions, which assumes additivity of the scattering phases on different bound nucleons. This is a single-channel approximation assuming that absorption, that is, inelastic interactions, generates via the unitarity relation only elastic scattering. In reality, diffractive excitations of hadrons frequently happen, and the Glauber approach was generalized to a multichannel case by Gribov [2]. The corresponding corrections to the Glauber approximation are known as inelastic shadowing or Gribov corrections. Unfortunately, the multichannel problem needs detailed experimental information, which is mostly unknown. One has to know all diffractive amplitudes, diagonal and off-diagonal, for different diffractive excitations of the hadron. Even the lowest order correction contains an unknown attenuation factor for an excited state propagating through the nucleus [3].

One can sum up the Gribov corrections to all orders by switching to the interaction eigenstates [4], which were identified in Ref. [5] as color dipoles and where the dipole approach to high-energy collisions was proposed. This phenomenology needs lesser input, and the key ingredient, the dipole-nucleon cross section, is flavor-independent and can be studied in different processes.

This method can be applied also to lepton- or photon-nucleus collisions [6–8], where leptons and photons dis-

play hadronic properties. A detailed study of the inelastic shadowing corrections to different diffractive channels in proton-nucleus collisions was performed, within the dipole approach, in Refs. [9,10].

Here we are going to enhance the accuracy of the calculations presented in Ref. [10] by improving the model for the nuclear wave function. Namely, most of calculations for nuclear shadowing effects have relied so far on a simplified model of an uncorrelated single-particle density distribution in the nucleus. This model, in particular, ignores the well-known experimental evidence for the existence of a strong repulsion core between nucleons. Such a repulsion should lead to short-range NN correlations in the nuclear density function, which in turn should modify the effective nuclear thickness function controlling diffractive processes.

The consideration of possible effects from nucleon-nucleon (NN) short-range correlations (SRC) appears to be particularly interesting in view of recent experimental data on lepton and hadron scattering off nuclei at medium energy, which provided quantitative evidence on SRC and their possible effects on dense hadronic matter [11]. Moreover, a recent calculation of the total neutron-nucleus cross section at Fermilab energies has indeed shown relevant effects from SRC even at high energies [12].

II. GLAUBER FORMALISM

The key assumption of the Glauber model is that the hadron-nucleus partial elastic amplitude at impact parameter b has the eikonal form [1]

$$\Gamma^{pA}(\vec{b}; \{\vec{l}_j, z_j\}) = 1 - \prod_{k=1}^A [1 - \Gamma^{pN}(\vec{b} - \vec{l}_k)], \quad (1)$$

where $\{\vec{l}_j, z_j\}$ denotes the coordinates of an i th target nucleon; $i\Gamma^{pN}$ is the elastic scattering amplitude on a nucleon, normalized as

$$\sigma_{\text{tot}}^{pN} = 2 \int d^2b \text{Re}\Gamma^{pN}(b). \quad (2)$$

Furthermore, one should calculate the matrix element of the amplitude [Eq. (1)] with the nuclear wave function, $\psi_0(\vec{r}_1, \vec{r}_2, \dots, \vec{r}_A) = \psi_0(\{\vec{r}_j\}) \equiv |0\rangle$. Here we introduce new notations,

$$\begin{aligned} G_A(\vec{b}) &= \langle 0 | \Gamma^{pA}(\vec{b}; \{\vec{l}_j, z_j\}) | 0 \rangle \\ &= 1 - \langle 0 | \prod_{i=1}^A G^{pN}(\vec{b} - \vec{l}_i) | 0 \rangle, \end{aligned} \quad (3)$$

where

$$G^{pN}(\vec{b} - \vec{l}_i) = 1 - \Gamma^{pN}(\vec{b} - \vec{l}_i). \quad (4)$$

The main problem in evaluating nuclear effects is therefore the choice of the nuclear wave function $\psi_0(1, \dots, A)$.

A. Single-particle approximation for the nuclear wave function

The most popular model for the square of the nuclear wave function appearing in the Glauber formalism is the approximation of single-particle nuclear density,¹

$$|\Psi_A(\vec{r}_1, \dots, \vec{r}_A)|^2 \simeq \prod_{j=1}^A \rho_A(\vec{l}_j, z_j), \quad (5)$$

where

$$\rho_A(\vec{l}_1, z_1) = \int \prod_{i=2}^A d^3r_i |\Psi_A(\{\vec{r}_j\})|^2. \quad (6)$$

Within such an approximation, the matrix element between the nuclear ground states reads

$$\begin{aligned} \langle 0 | \Gamma^{pA}(\vec{b}; \{\vec{l}_j, z_j\}) | 0 \rangle \\ = 1 - \left[1 - \frac{1}{A} \int d^2l \Gamma^{pN}(l) \int_{-\infty}^{\infty} dz \rho_A(\vec{b} - \vec{l}, z) \right]^A. \end{aligned} \quad (7)$$

Correspondingly, the total pA cross section has the form

$$\begin{aligned} \sigma_{\text{tot}}^{pA} &= 2\text{Re} \int d^2b \left\{ 1 - \left[1 - \frac{1}{A} \int d^2l \Gamma^{pN}(l) T_A(\vec{b} - \vec{l}) \right]^A \right\} \\ &\approx 2 \int d^2b \times \left\{ 1 - \exp \left[-\frac{1}{2} \sigma_{\text{tot}}^{pN} (1 - i\alpha_{pN}) T_A^h(b) \right] \right\}, \end{aligned} \quad (8)$$

where α_{pN} is the ratio of the real to imaginary parts of the forward pN elastic amplitude,

$$T_A^h(b) = \frac{2}{\sigma_{\text{tot}}^{pN}} \int d^2l \text{Re}\Gamma^{pN}(l) T_A(\vec{b} - \vec{l}), \quad (9)$$

¹We ignore the effect of motion of the center of gravity, assuming the nucleus to be sufficiently heavy.

and

$$T_A(b) = \int_{-\infty}^{\infty} dz \rho_A(b, z) \quad (10)$$

is the nuclear thickness function. We use the Gaussian form of $\Gamma^{pN}(l)$:

$$\text{Re}\Gamma^{pN}(l) = \frac{\sigma_{\text{tot}}^{pN}}{4\pi B_{\text{el}}^{pN}} \exp\left(\frac{-l^2}{2B_{\text{el}}^{pN}}\right). \quad (11)$$

Notice that in Eq. (8) and in what follows, we use the exponential approximation of large A only to simplify and clarify the formulas. For numerical calculations throughout the article, we always rely on the exact expressions such as the first part of Eq. (8).

The Glauber approach is a single-channel model, and therefore it is unable to consider diffractive excitation of the proton. However, a part of diffractive excitation of the nucleus occurs without excitation of the bound nucleons, when the nucleus just breaks up into free nucleons and nuclear fragments. Such events, $pA \rightarrow pF$, are called quasielastic and can be calculated within the Glauber approximation. Summing up the final states of the nucleus $|F\rangle$, applying the condition of completeness, and extracting the contribution of the ground state of the nucleus, one gets

$$\begin{aligned} \sigma_{\text{qel}}^{pA} &\equiv \sum_F \sigma(pA \rightarrow pF) - \sigma_{\text{el}}^{pA} \\ &= \sum_F \int d^2b [\langle 0 | \Gamma^{pA}(b) | F \rangle^\dagger \langle F | \Gamma^{pA}(b) | 0 \rangle \\ &\quad - | \langle 0 | \Gamma^{pA}(b) | 0 \rangle |^2] \\ &= \int d^2b [\langle 0 | \Gamma^{pA}(b) |^2 | 0 \rangle - | \langle 0 | \Gamma^{pA}(b) | 0 \rangle |^2]. \end{aligned} \quad (12)$$

In the first order in nuclear density, the first term in this expression, $\langle 0 | \Gamma^{pA}(b) |^2 | 0 \rangle$, contains, besides the usual linear term [Eq. (9)], the quadratic term $\int d^2s T_A(\vec{b} - \vec{l}) [\Gamma^{pN}(l)]^2 = T_A^h(b) \sigma_{\text{el}}^{pN}$. Both terms together result in the exponent $\sigma_{\text{in}}^{pN} T_A(b)$. Then the quasielastic cross section gets the form

$$\begin{aligned} \sigma_{\text{qel}}^{pA}(pA \rightarrow pA^*) \\ = \int d^2b \{ \exp[-\sigma_{\text{in}}^{pN} T_A^h(b)] - \exp[-\sigma_{\text{tot}}^{pN} T_A^h(b)] \}. \end{aligned} \quad (13)$$

B. Nucleon correlations

Equation (5) represents only the lowest order term of the square of the full nuclear wave function $|\psi_0|^2$. As a matter of fact, the latter can be written as an expansion in terms of density matrices [1,13], as follows:

$$\begin{aligned} |\psi_0(\vec{r}_1, \dots, \vec{r}_A)|^2 &= \prod_{j=1}^A \rho_1(\vec{r}_j) + \sum_{i < j} \Delta(\vec{r}_i, \vec{r}_j) \prod_{k \neq i, j} \rho_1(\vec{r}_k) \\ &\quad + \sum_{(i < j) \neq (k < l)} \Delta(\vec{r}_i, \vec{r}_j) \Delta(\vec{r}_k, \vec{r}_l) \\ &\quad \times \prod_{m \neq i, j, k, l} \rho_1(\vec{r}_m) + \dots, \end{aligned} \quad (14)$$

in which the single-particle density $\rho_1(\vec{r}_i)$ is (e.g. $i = 1$)

$$\rho_1(\vec{r}_1) = \int |\psi_o(\vec{r}_1, \vec{r}_2, \dots, \vec{r}_A)|^2 \prod_{i=2}^A d^3 r_i \quad (15)$$

and the two-body contraction Δ is

$$\Delta(\vec{r}_i, \vec{r}_j) = \rho_2(\vec{r}_i, \vec{r}_j) - \rho_1(\vec{r}_i)\rho_1(\vec{r}_j). \quad (16)$$

The two-body density matrix

$$\rho_2(\vec{r}_1, \vec{r}_2) = \int |\psi_o(\vec{r}_1, \vec{r}_2, \dots, \vec{r}_A)|^2 \prod_{i=3}^A d^3 r_i \quad (17)$$

satisfies the sequential condition

$$\int d^3 r_j \rho_2(\vec{r}_i, \vec{r}_j) = \rho_1(\vec{r}_i), \quad (18)$$

which leads to the basic property of the two-body contraction:

$$\int d^3 r_j \Delta(\vec{r}_i, \vec{r}_j) = 0. \quad (19)$$

Notice that the single-particle density appearing in Eq. (14) is normalized to 1 so that the densities defined by Eq. (6) and Eq. (15) are simply related by $\rho_A(\vec{r}) = A\rho_1(\vec{r})$. It should be stressed that in Eq. (14), only unlinked contractions have to be considered, and that the higher order terms, not explicitly displayed, include unlinked products of 3, 4, and so on, two-body contractions, representing contributions to two-nucleon correlations, and unlinked products of three-body, four-body, and so on, contractions, describing three-nucleon, four-nucleon, and so on, correlations. We will give now a short derivation of the total cross section, including two-nucleon correlations (more details will be given elsewhere [14]). Taking into account all terms of the expansion [Eq. (14)] containing all possible numbers of unlinked two-body contractions, Eq. (3) can be written in the following form, which yields the usual Glauber profile when $\Delta = 0$ [12,14]:

$$\begin{aligned} G_A(b) &\equiv \int \prod_{k=1}^A d^3 r_k |\psi_o(1 \dots A)|^2 \prod_{i=1}^A G^{pN}(\vec{b} - \vec{l}_i) \\ &= \int \prod_{k=1}^A d^3 r_k \rho_1(\vec{r}_k) G^{pN}(\vec{b} - \vec{l}_k) \\ &+ \sum_{i < j} \int \prod_{k=1}^A d^3 r_k \Delta(\vec{r}_i, \vec{r}_j) \prod_{l \neq i, j} \rho_1(\vec{r}_l) G^{pN}(\vec{b} - \vec{l}_k) \\ &+ \sum_{i < j \neq p < l} \int \prod_{k=1}^A d^3 r_k \Delta(\vec{r}_i, \vec{r}_j) \Delta(\vec{r}_p, \vec{r}_l) \\ &\times \prod_{m \neq i, j, p, l}^A \rho_1(\vec{r}_m) G^{pN}(\vec{b} - \vec{l}_k) + \dots \\ &= G_A^{(0)}(\vec{b}) + G_A^{(1)}(\vec{b}) + G_A^{(2)}(\vec{b}) + \dots, \quad (20) \end{aligned}$$

where the superscript denotes the number of two-body contractions in the given term, each term containing Glauber profiles to all orders. For each nucleus, we have considered all terms

of the series of Eq. (20), the first term, corresponding to the single-particle approximation of Eq. (5), being

$$\begin{aligned} G_A^{(0)}(b) &= \int \prod_{k=1}^A d^3 r_k \rho_1(\vec{r}_k) G^{pN}(\vec{b} - \vec{l}_k) \\ &= \left[1 - \frac{1}{A} \int d^3 r_1 \rho_A(\vec{r}_1) \Gamma^{pN}(\vec{b} - \vec{l}_1) \right]^A, \quad (21) \end{aligned}$$

and the n th term being

$$G_A^{(n)}(b) = \frac{A!}{2^n n! (A - 2n)!} X^n(b) Y^{A-2n}(b), \quad (22)$$

where

$$X(b) = \int d^3 r_1 d^3 r_2 \Delta(\vec{r}_1, \vec{r}_2) \Gamma^{pN}(\vec{b} - \vec{l}_1) \Gamma^{pN}(\vec{b} - \vec{l}_2) \quad (23)$$

and

$$Y(b) = \left[1 - \frac{1}{A} \int d^3 r_1 \rho_A(\vec{r}_1) \Gamma^{pN}(\vec{b} - \vec{l}_1) \right], \quad (24)$$

resulting from the basic properties of the two-body contraction: $\int d^3 r_{i,j} \Delta(\vec{r}_i, \vec{r}_j) = 0$ and

$$\begin{aligned} &\int d^3 r_1 d^3 r_2 \Delta(\vec{r}_1, \vec{r}_2) G^{pN}(\vec{b} - \vec{l}_1) G^{pN}(\vec{b} - \vec{l}_2) \\ &= \int d^3 r_1 d^3 r_2 \Delta(\vec{r}_1, \vec{r}_2) \Gamma^{pN}(\vec{b} - \vec{l}_1) \Gamma^{pN}(\vec{b} - \vec{l}_2). \quad (25) \end{aligned}$$

Equation (20) can now be written as follows:

$$\begin{aligned} G_A(b) &= \sum_{n=0}^{A/2} \frac{A! X^n(b) [Y(b)]^{A-2n}}{2^n n! (A - 2n)!} \xrightarrow{A \gg 1} [Y(b)]^A \\ &\times \sum_{n=0}^{\infty} \frac{A^{2n} X^n(b)}{2^n n!} = [Y(b)]^A e^{\frac{A^2}{2} X(b)}. \quad (26) \end{aligned}$$

Using, for ease of presentation, the optical limit approximation

$$\begin{aligned} [Y(b)]^A &= \left[1 - \frac{1}{A} \int d^3 r_1 \rho_1(\vec{r}_1) \Gamma^{pN}(\vec{b} - \vec{l}_1) \right]^A \\ &= e^{-\int d^3 r_1 \rho_A(\vec{r}_1) \Gamma(\vec{b} - \vec{l}_1)}, \quad (27) \end{aligned}$$

the insertion of Eq. (27) into Eq. (26) leads to the final result:

$$\begin{aligned} G_A(b) &\simeq 1 - \exp \left[- \int d^3 r_1 \rho_A(\vec{r}_1) \Gamma(\vec{b} - \vec{l}_1) \right. \\ &\quad \left. + \frac{1}{2} \int d^3 r_1 d^3 r_2 \Delta_A(\vec{r}_1, \vec{r}_2) \Gamma(\vec{b} - \vec{l}_1) \Gamma(\vec{b} - \vec{l}_2) \right] \\ &= 1 - \exp \left[- \frac{1}{2} \sigma_{\text{tot}}^{pN} \tilde{T}_A^h(b) \right], \quad (28) \end{aligned}$$

where

$$\Delta_A(\vec{r}_1, \vec{r}_2) = \rho_A^{(2)}(\vec{r}_1, \vec{r}_2) - \rho_A(\vec{r}_1)\rho_A(\vec{r}_2), \quad (29)$$

which obviously differs from Eq. (16) simply by a factor A^2 , and

$$\tilde{T}_A^h(b) = T_A^h(b) - \Delta T_A^h(b), \quad (30)$$

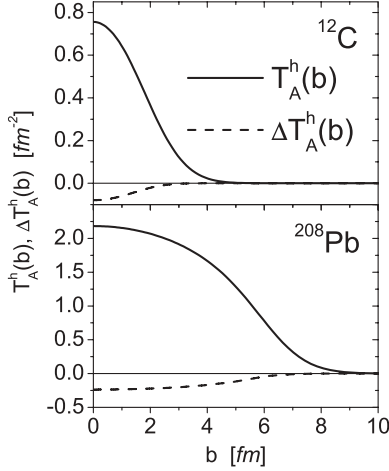


FIG. 1. Nuclear thickness function $T_A^h(b)$ and the correction owing to NN correlations, $\Delta T_A^h(b)$, calculated at the energy of HERA-B for (top) carbon and (bottom) lead.

with $T_A^h(b)$ given by Eq. (9) and

$$\Delta T_A^h(b) = \frac{(1 - i\alpha_{pN})}{\sigma_{\text{tot}}^{pN}} \int d^2l_1 d^2l_2 \Delta_A^\perp(\vec{l}_1, \vec{l}_2) \times \text{Re}\Gamma^{pN}(\vec{b} - \vec{l}_1) \text{Re}\Gamma^{pN}(\vec{b} - \vec{l}_2), \quad (31)$$

where

$$\Delta_A^\perp(\vec{l}_1, \vec{l}_2) = \int_{-\infty}^{\infty} dz_1 \int_{-\infty}^{\infty} dz_2 \Delta_A(\vec{r}_1, \vec{r}_2) \quad (32)$$

is the transverse two-nucleon contraction. It can be seen that the inclusion of NN correlations in nuclei leads to a modification of the nuclear thickness function $T_A^h(b) \Rightarrow \tilde{T}_A^h(b)$. Owing to its general structure and the basic property $\int d^3r_{1,2} \Delta_A(\vec{r}_1, \vec{r}_2) = 0$, the sign of the contraction is mostly negative, with a small positive contribution at large separations. In Fig. 1, we present $T_A^h(b)$ and $\Delta T_A^h(b)$ for ^{12}C and ^{208}Pb . We see that $\Delta T_A^h(b)$ is indeed mostly negative, so according to the definition of Eq. (30), correlations increase the nuclear thickness function and make the nuclear medium more opaque [12]. At the same time, the corrections are small, $\Delta T_A^h(b) \ll T_A^h(b)$, and the effects from higher order correlations, estimated in Ref. [12], can safely be disregarded.

A short description of the way in which the one- and two-body densities and contractions have been calculated is now in order. Following Ref. [12], the two-body density has been obtained from the fully correlated wave function of Refs. [15,16], $\psi_0 = \hat{F}\phi_0$, where $\hat{F} = \prod_{i<j} [\sum_{k=1}^8 f_k(r_{ij}) \hat{O}_k(ij)]$ is a correlation operator generated by the realistic Argonne V8' interaction [17] and ϕ_0 is a mean-field shell-model wave function composed of Woods-Saxon single-particle orbitals. The preceding wave function largely differs from the Jastrow one, featuring only central correlations, because the operator \hat{F} generates central ($\hat{O}_1 = 1$), spin [$\hat{O}_2(ij) = \vec{\sigma}_i \cdot \vec{\sigma}_j$], isospin [$\hat{O}_3(ij) = \vec{\tau}_i \cdot \vec{\tau}_j$], spin-isospin [$\hat{O}_4(ij) = (\vec{\sigma}_i \cdot \vec{\sigma}_j)(\vec{\tau}_i \cdot \vec{\tau}_j)$], tensor [$\hat{O}_5(ij) = \vec{S}_{ij}$], tensor-isospin [$\hat{O}_6(ij) = \vec{S}_{ij}(\vec{\tau}_i \cdot \vec{\tau}_j)$], and so on, correlations. The two-body density and contraction therefore reflect not only the short-range repulsion but also the spin-isospin dependence of the interaction, particularly

that generated by the tensor force. The parameters of both the single-particle wave functions and the various correlation functions have been fixed from the ground-state energy calculation so that no free parameters are present in our approach.

The contraction $\Delta(\vec{r}_1, \vec{r}_2)$ resulting from our calculation exactly satisfies the sum rule $\int d^3r_1 \Delta(\vec{r}_1, \vec{r}_2) = 0$ because the one-body density $\rho_1(\vec{r}_1)$ exactly results from the integration of $\rho_2(\vec{r}_1, \vec{r}_2)$. Notice, moreover, that our one-body point density and radii are in agreement with electron scattering data [18]. We have also investigated the validity of the approximation in which the nuclear matter two-body density $\rho_2(\vec{r}_1, \vec{r}_2) = \rho_1(\vec{r}_1)\rho_1(\vec{r}_2)g(|\vec{r}_1 - \vec{r}_2|)$ is used for finite nuclei, finding that it leads to a strong violation of the sequential relation $\int d^3r \rho_2(\vec{r}_1, \vec{r}_2) = \rho_1(\vec{r}_1)$ for nuclei with $A < 208$. Thus, when such an approximation is used to introduce correlations in light- and medium-weight nuclei, a mismatch between the one-body density (usually taken from the experimental data) and the two-body density is generated.

Using the nuclear thickness function, which includes the effects of correlations [Eq. (30)], the total cross section [Eq. (8)] acquires a correction, $\sigma_{\text{tot}}^{pA} \Rightarrow \sigma_{\text{tot}}^{pA} + \Delta\sigma_{\text{tot}}^{pA}$, which is positive and can be approximated as

$$\Delta\sigma_{\text{tot}}^{pA} \approx -\sigma_{\text{tot}}^{pN} \int d^2b \Delta T_A^h(b) \exp\left[-\frac{1}{2}\sigma_{\text{tot}}^{pN} T_A^h(b)\right], \quad (33)$$

which is also positive because $\Delta T_A^h(b)$ is itself negative.

We see that this correction to the total cross section comes mainly from peripheral collisions and rises with A rather slowly, as $A^{1/3}$. Notice that the accuracy of the optical (exponential) approximation in Eq. (8) is quite good, $\sim 10^{-3}$ for heavy nuclei, but it gets worse with decreasing A , and therefore for numerical calculations, as was already mentioned, we rely on the exact Glauber expressions throughout the article. In what follows, we neglect the real part of the elastic amplitude, which gives quite a small correction, $\sim \rho_{\text{pp}}^2/A^{2/3}$, and which otherwise can be easily implemented.

The simplest process with a large rapidity gap (LRG) is elastic scattering. It is worth noting, however, that this channel is enhanced by absorptive corrections, whereas other LRG processes considered later are suppressed by these corrections.

The elastic cross section according to Eq. (7) reads

$$\sigma_{\text{el}}^{pA} = \int d^2b \left| 1 - \exp\left[-\frac{1}{2}\sigma_{\text{tot}}^{pN} \tilde{T}_A^h(b)\right] \right|^2, \quad (34)$$

where $\tilde{T}_A^h(b)$ is given by Eq. (30).

The quasielastic cross section also gets modifications compared to the Glauber expression [Eq. (13)]. The nucleon correlations show up in the second order in nuclear density, leading to an additional term proportional to $(\sigma_{\text{in}}^{pN})^2 \Delta T_A^h(b)$. Thus the cross section of quasielastic proton-nucleus scattering, $pA \rightarrow pA^*$, gets the form

$$\sigma_{\text{qel}}^{pA} = \int d^2b \left\{ \exp\left[-\sigma_{\text{in}}^{pN} T_A^h(b) - \frac{(\sigma_{\text{in}}^{pN})^2}{\sigma_{\text{tot}}^{pN}} \Delta T_A^h(b)\right] - \exp\left[-\sigma_{\text{tot}}^{pN} (T_A^h(b) + \Delta T_A^h(b))\right] \right\}. \quad (35)$$

Notice that in deriving this expression, we implicitly used the assumption that the impact parameter dependence of powers of the amplitude $\Gamma^{pN}(s)$ does not depend on the power. Although this is certainly not correct, the approximation is rather accurate as far as the NN interaction radius is much smaller than the size of the nucleus. Nevertheless, we used this approximation only for the sake of clarity and simplicity. For numerical calculations, we use the more complicated but exact analog of Eq. (35).

III. GRIBOV CORRECTIONS VIA LIGHT-CONE DIPOLES

The dipole representation for the amplitude of hadronic interactions allows us to sum the Gribov inelastic corrections to all orders. We assume the collision energy to be high enough to keep the dipole size “frozen” by Lorentz time dilation during propagation through the nucleus. In this limit, the calculations are much simplified.

The key ingredients of the approach are the universal dipole-nucleon cross section and the light-cone wave function of the projectile hadron [5]. Several different models were tested in Ref. [10] by comparing with data on proton diffraction. Here we select two models that describe diffraction quite well. Both employ the saturated shape of the dipole cross section and differ only by modeling the proton wave function.

In the limit of soft interactions, the Bjorken x is no longer a proper variable, and the dipole cross section should depend on energy. We rely on the model proposed in Ref. [19] and fitted to data:

$$\sigma_{\bar{q}q}(r_T, s) = \sigma_0(s) \left[1 - \exp\left(-\frac{r_T^2}{R_0^2(s)}\right) \right], \quad (36)$$

where $R_0(s) = 0.88 \text{ fm } (s_0/s)^{0.14}$ and $s_0 = 1000 \text{ GeV}^2$ [19]. The energy-dependent factor $\sigma_0(s)$ is defined as

$$\sigma_0(s) = \sigma_{\text{tot}}^{\pi p}(s) \left(1 + \frac{3R_0^2(s)}{8\langle r_{\text{ch}}^2 \rangle_{\pi}} \right), \quad (37)$$

where $\langle r_{\text{ch}}^2 \rangle_{\pi} = 0.44 \pm 0.01 \text{ fm}^2$ [20] is the mean square of the pion charge radius. This dipole cross section is normalized to reproduce the pion-proton total cross section, $\langle \sigma_{\bar{q}q} \rangle_{\pi} = \sigma_{\text{tot}}^{\pi p}(s)$.

For the proton wave function, we employ two models.

A. $q - 2q$ model

There is much evidence (although none looks decisive) for a strong pairing of the u and d valence quarks into a small-size scalar-isoscalar diquark [21–23]. Neglecting the diquark radius, we arrive at a meson-type color dipole structure of the proton:

$$|\Psi_N(\vec{r}_1, \vec{r}_2, \vec{r}_3)|^2 = \frac{2}{\pi R_p^2} \exp\left(-\frac{2r_T^2}{R_p^2}\right), \quad (38)$$

where \vec{r}_i are the interquark transverse distances, $\vec{r}_3 = 0$, $\vec{r}_T = \vec{r}_1 = \vec{r}_2$, and R_p is related to the mean charge radius squared of the proton as $R_p^2 = \frac{16}{3}\langle r_{\text{ch}}^2 \rangle_p$. The dipole wave function squared

[Eq. (38)] convoluted with the dipole cross section [Eq. (36)] gives the proton-proton total cross section.

In this model, the effect of the Gribov corrections in all orders is equivalent to the replacement of the Glauber formula [Eq. (8)] by

$$\begin{aligned} \sigma_{\text{tot}}^{pA} &= 2 \int d^2b \int_0^1 d\alpha \int d^2r_T |\Psi_N(r_T, \alpha)|^2 \\ &\quad \times \left[1 - e^{-\frac{1}{2}\sigma_{\bar{q}q}(r_T, s)T_A^{\bar{q}q}(b, r_T, \alpha)} \right] \\ &\equiv 2 \int d^2b \left[1 - \langle e^{-\frac{1}{2}\sigma_{\bar{q}q}(r_T, s)T_A^{\bar{q}q}(b, r_T, \alpha)} \rangle \right]. \end{aligned} \quad (39)$$

Here we consider a $\bar{q}q$ (or qq - q) dipole of transverse separation \vec{r}_T and fractional light-cone momenta α and $1 - \alpha$ of the constituents. The integration over these variables weighted by the hadron wave function squared is denoted as averaging. The new notation, $T_A^{\bar{q}q}(b, r_T, \alpha)$, is

$$T_A^{\bar{q}q}(b, r_T, \alpha) = \frac{2}{\sigma_{\bar{q}q}(r_T)} \int d^2l \text{Re}\Gamma^{\bar{q}qN}(\vec{l}, \vec{r}_T, \alpha) T_A(\vec{b} - \vec{l}). \quad (40)$$

The partial dipole-nucleon elastic amplitude $\text{Re}\Gamma^{\bar{q}qN}(\vec{l}, r_T, \alpha)$, corresponding to the dipole cross section of Eq. (36), was derived recently in Refs. [24–26]:

$$\begin{aligned} \text{Re}\Gamma^{\bar{q}qN}(\vec{l}, \vec{r}_T, \alpha) &= \frac{\sigma_0(s)}{8\pi B(s)} \left\{ \exp\left[-\frac{[\vec{l} + \vec{r}_T(1 - \alpha)]^2}{2B(s)}\right] \right. \\ &\quad + \exp\left[-\frac{(\vec{l} - \vec{r}_T\alpha)^2}{2B(s)}\right] - 2 \exp\left[-\frac{r_T^2}{R_0^2(s)}\right] \\ &\quad \left. - \frac{[\vec{l} + (1/2 - \alpha)\vec{r}_T]^2}{2B(s)} \right\}, \end{aligned} \quad (41)$$

where $B(s) = B_{\text{el}}^{pN}(s) - \frac{1}{3}\langle r_{\text{ch}}^2 \rangle_p - 1/8R_0^2(s)$. It is easy to check that this partial amplitude correctly reproduces the dipole-nucleon cross section [Eq. (36)],

$$\sigma_{\bar{q}q}(r_T, s) = 2 \int d^2l \text{Re}\Gamma^{\bar{q}qN}(\vec{l}, \vec{r}_T, \alpha), \quad (42)$$

and the slope of the differential elastic pN scattering,

$$B_{\text{el}}^{pN}(s) = \frac{1}{\sigma_{\text{tot}}^{pN}} \int d^2l l^2 \langle \text{Re}\Gamma^{\bar{q}qN}(\vec{l}, \vec{r}_T, \alpha) \rangle. \quad (43)$$

These properties of the partial amplitude lead to the following relations, with the analogous functions defined previously within the Glauber model:

$$\sigma_{\text{tot}}^{pN} = \langle \sigma_{\bar{q}q}(r_T) \rangle, \quad (44)$$

$$\text{Re}\Gamma^{pN}(l) = \langle \text{Re}\Gamma^{\bar{q}qN}(\vec{l}, \vec{r}_T, \alpha) \rangle, \quad (45)$$

$$T_A^h(b) = \frac{1}{\sigma_{\text{tot}}^{pN}} \langle \sigma_{\bar{q}q}(r_T) T_A^{\bar{q}q}(b, r_T, \alpha) \rangle. \quad (46)$$

Thus the difference between the Glauber formula [Eq. (8)] and the exact expression [Eq. (39)] is in how the averaging over r_T and α is done: In the former case, the averaging is done in the exponent, whereas in the latter case, the whole exponential is averaged.

Notice that $T_A^{\bar{q}q}(b, r_T, \alpha)$ in the exponent in Eq. (39) can be replaced by $T_A^h(b)$ with high precision. Indeed, at small $r_T^2 \ll R_0^2(s)$, the partial amplitude [Eq. (41)] vanishes as $\text{Re}\Gamma^{\bar{q}qN}(\vec{l}, \vec{r}_T, \alpha) \propto r_T^2$. This r_T dependence cancels in Eq. (40) with the same behavior of $\sigma_{\bar{q}q}(r_T)$ in the denominator. Thus $T_A^{\bar{q}q}(b, r_T, \alpha)$ is independent of r_T in this limit. In the opposite limit of large $r_T^2 \gg R_0^2(s)$, the last term in Eq. (39) vanishes, and the amplitude integrated over d^2l becomes a constant. Moreover, the denominator of Eq. (40) is independent of r_T in this limit. Thus one can neglect the slow r_T dependence of $T_A^{\bar{q}q}(b, r_T, \alpha)$ in Eq. (46) in comparison with the fast-varying function $\sigma_{\bar{q}q}(r_T)$, which is equivalent to the replacement $T_A^{\bar{q}q}(b, r_T, \alpha) \Rightarrow T_A^h(b)$. We rely on this approximation in Eq. (39) and in what follows.

Thus, for the total p - A cross section, we recover the standard expression [5,10]

$$\sigma_{\text{tot}}^{pA} = 2 \int d^2b \int d^2r_T |\Psi_N(r_T)|^2 \times \left\{ 1 - \exp \left[-\frac{1}{2} \sigma_{\bar{q}q}(r_T, s) T_A^h(b) \right] \right\}. \quad (47)$$

B. 3 q model

Another extreme is to assume no pairing forces and a symmetric valence quark wave function:

$$|\Psi_N(\vec{r}_1, \vec{r}_2, \vec{r}_3)|^2 = \frac{3}{(\pi R_p^2)^2} \delta(\vec{r}_1 + \vec{r}_2 + \vec{r}_3) \times \exp \left(-\frac{r_1^2 + r_2^2 + r_3^2}{R_p^2} \right). \quad (48)$$

Here the mean interquark separation squared is $\langle \vec{r}_i^2 \rangle = 2/3 R_p^2 = 2 \langle r_{\text{ch}}^2 \rangle_p$. In this case, one needs a cross section for a three-quark dipole, $\sigma_{3q}(\vec{r}_1, \vec{r}_2, \vec{r}_3)$, where \vec{r}_i are the transverse quark separation, with the condition $\vec{r}_1 + \vec{r}_2 + \vec{r}_3 = 0$. To avoid the introduction of a new unknown phenomenological quantity, we express the three-body dipole cross section via the conventional dipole cross section $\sigma_{\bar{q}q}$ [9,10]:

$$\sigma_{3q}(\vec{r}_1, \vec{r}_2, \vec{r}_3) = \frac{1}{2} [\sigma_{\bar{q}q}(r_1) + \sigma_{\bar{q}q}(r_2) + \sigma_{\bar{q}q}(r_3)]. \quad (49)$$

This form satisfies the limiting conditions, namely, turning into $\sigma_{\bar{q}q}(r)$ if one of three separations is zero. It is also confirmed well by perturbative calculations [27].

In this model, the Gribov corrections modify the Glauber expression [Eq. (8)] as

$$\sigma_{\text{tot}}^{pA} = 2 \int d^2b \int d^2r_1 d^2r_2 d^2r_3 |\Psi_N(r_i)|^2 \times \left\{ 1 - \exp \left[-\frac{1}{2} \sigma_{3q}(r_i, s) T_A^h(b) \right] \right\}. \quad (50)$$

IV. GRIBOV CORRECTIONS TO THE EFFECT OF NN CORRELATIONS

Nucleon correlations lead to further modifications of the exponent in Eq. (39), which correspond to the replacement

$T_A^{\bar{q}q}(b, r_T, \alpha) \Rightarrow T_A^{\bar{q}q}(b, r_T, \alpha) + \Delta T_A^{\bar{q}q}(b)$, where

$$\Delta T_A^{\bar{q}q}(b, r_T, \alpha) = \frac{1}{\sigma_{\bar{q}q}(r_T)} \int d^2l_1 d^2l_2 \Delta_A^\perp(\vec{l}_1, \vec{l}_2) \times \text{Re} \Gamma^{\bar{q}q}(\vec{b} - \vec{l}_1, r_T, \alpha) \text{Re} \Gamma^{\bar{q}q}(\vec{b} - \vec{l}_2, r_T, \alpha). \quad (51)$$

Changing the integration variables $d^2l_1 d^2l_2 \Rightarrow d^2L d^2\delta$, where

$$\begin{aligned} \vec{L} &= (\vec{l}_1 + \vec{l}_2)/2, \\ \vec{\delta} &= \vec{l}_1 - \vec{l}_2, \end{aligned} \quad (52)$$

one has, correspondingly, $\Delta_A^\perp(\vec{l}_1, \vec{l}_2) \Rightarrow \Delta_A^\perp(\vec{L}, \vec{\delta})$. This function is rather smooth and varies over distances much longer than the interaction radius. Therefore we can take it out of the integral in Eq. (51), fixing it at $\vec{L} = \vec{b}$. Then, using the partial amplitude [Eq. (41)], one can perform the integration over d^2L in Eq. (51) and then average over r_T and α . The result is

$$\begin{aligned} &\int d^2L (\text{Re} \Gamma^{\bar{q}q}(\vec{l}_1, r_T, \alpha) \text{Re} \Gamma^{\bar{q}q}(\vec{l}_2, r_T, \alpha)) \\ &= [\sigma_{\text{el}}^{pN} + \sigma_{\text{sd}}^{pN}] \exp \left[-\frac{\delta^2}{4B(s) + R_0^2(s)/2} \right]. \end{aligned} \quad (53)$$

Here σ_{sd}^{pN} is the single-diffraction cross section, $pN \rightarrow XN$, and the relation [5,10,28]

$$\int d^2L (\text{Re} \Gamma^{\bar{q}q}(\vec{L}, r_T, \alpha))^2 = \sigma_{\text{el}}^{pN} + \sigma_{\text{sd}}^{pN} \quad (54)$$

has been used. Data show that at high energies, this cross section is nearly constant and is about $\sigma_{\text{sd}}^{pN} \approx 4$ mb, the value we use in what follows.

Notice that data for single diffraction also include the contribution from the triple-Pomeron term, which corresponds to diffractive gluon radiation. This term has not been included so far in our calculations, which correspond only to diffractive excitation of the valence quark skeleton of the proton (see Ref. [10]). However, the higher Fock components of the light-cone wave function of the proton should be also added, which effectively incorporate this contribution by using the total single-diffraction cross section.

Equation (53) turns into the Glauber model relation Eq. (31) if the diffraction term is removed and the denominator of the exponent is replaced by $4B_{\text{el}}^{pN}$. Eventually, the correction related to the nucleon correlations to the nuclear thickness function, convoluted with the dipole cross section, takes the form

$$\begin{aligned} I_A(b) &= \langle \sigma_{\bar{q}q}(r_T) \Delta T_A^{\bar{q}q}(b, r_T, \alpha) \rangle = [\sigma_{\text{el}}^{pN} + \sigma_{\text{sd}}^{pN}] \\ &\times \int d^2\delta \exp \left[-\frac{\delta^2}{4B(s) + R_0^2(s)/2} \right] \Delta_A^\perp(\vec{\delta}, b). \end{aligned} \quad (55)$$

The quantity $I_A(b)$ is shown in Fig. 2 for both ^{12}C and ^{208}Pb .

Because ΔT_A is small and its higher orders are negligible, there is no difference between averaging of the exponential

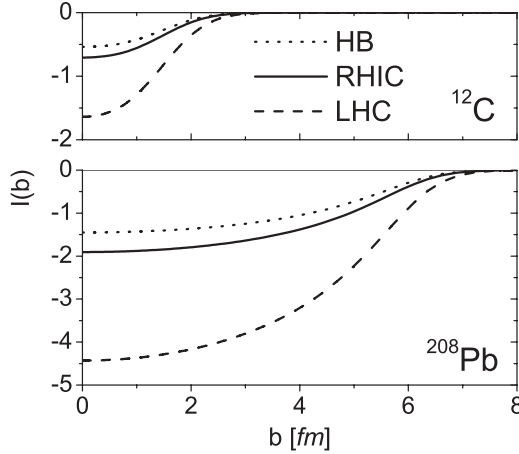


FIG. 2. The integral of Eq. (55) for (top) carbon and (bottom) lead, calculated at HERA-B (dotted lines), RHIC (solid lines), and LHC (dashed lines) energies.

and its exponent. Therefore the result [Eq. (55)] accounts for all inelastic shadowing effects in NN correlations. Then the total cross section reads

$$\sigma_{\text{tot}}^{pA} = 2 \int d^2b \left\{ 1 - e^{\frac{1}{2}I_A(b)} \left\langle e^{-\frac{1}{2}\sigma_{\text{dip}}T_A^n(b)} \right\rangle \right\}. \quad (56)$$

Here we use notation that unifies the two models under consideration; σ_{dip} is the dipole cross section, and averaging corresponds to integration over the light-cone momenta of the quarks, weighted with the proton wave function squared.

The results of the calculation of the total, elastic, and quasielastic cross sections for several nuclei and Hadron-Electron Ring Accelerator (HERA)-B, Relativistic Heavy Ion Collider (RHIC), and Large Hadron Collider (LHC) energies, obtained within the Glauber approach including NN correlations, are presented in Tables I, II, and III, respectively.

In our calculations, nuclear densities that give the correct nuclear rms radius have been adopted, and this is a reason for some differences compared to the results of Ref. [10] in the case of Glauber calculations. The parameters for the total nucleon-nucleon cross section and the slope of the Glauber profiles have been obtained as in Ref. [10]

V. DIFFRACTIVE EXCITATION OF THE PROTON IN pA COLLISIONS

Whereas the Glauber model, which is a single-channel approximation, cannot go beyond elastic scattering, the dipole approach treats diagonal and off-diagonal diffractive channels on the same footing. Although the calculation of exclusive channels of diffractive excitation needs knowledge of the light-cone wave function of the final state (e.g., see Refs. [29,30]), the total cross section of diffractive excitation summed over final states is easier to obtain because one can employ completeness.

Following the standard classification of diffractive channels in terms of the triple Regge approach [31], one can consider diffractive excitation of the valence quark system, which corresponds to the Pomeron-Pomeron-Reggeon ($IP\bar{P}R$)

TABLE I. HERA-B.

	Glauber	Glauber + SRC	q -2 q model + SRC	3 q model + SRC
^{12}C				
σ_{tot}	353.71	364.11	344.16	349.37
σ_{el}	86.90	92.96	82.39	85.42
σ_{sd}	—	—	5.43	2.40
$\sigma_{\text{sd}+\text{g}}$	—	—	0.07	0.06
σ_{qe}	22.85	19.62	21.12	22.05
σ_{qsd}	—	—	1.94	0.84
σ_{tsd}	—	—	12.47	12.92
σ_{dd}	—	—	0.61	0.26
^{27}Al				
σ_{tot}	697.32	714.35	675.93	688.08
σ_{el}	201.02	212.26	188.22	196.28
σ_{sd}	—	—	10.82	4.56
$\sigma_{\text{sd}+\text{g}}$	—	—	0.12	0.11
σ_{qe}	36.39	31.75	33.24	34.86
σ_{qsd}	—	—	2.92	1.23
σ_{tsd}	—	—	19.47	20.42
σ_{dd}	—	—	0.91	0.38
^{48}Ti				
σ_{tot}	1113.52	1135.53	1074.67	1095.93
σ_{el}	353.89	369.77	327.78	342.93
σ_{sd}	—	—	16.86	6.86
$\sigma_{\text{sd}+\text{g}}$	—	—	0.17	0.16
σ_{qe}	48.73	42.82	44.57	46.86
σ_{qsd}	—	—	3.85	1.61
σ_{tsd}	—	—	26.11	27.45
σ_{dd}	—	—	1.20	0.50
^{184}W				
σ_{tot}	2972.02	2986.46	2688.09	2747.66
σ_{el}	1174.09	1187.18	1025.16	1074.48
σ_{sd}	—	—	32.27	11.75
$\sigma_{\text{sd}+\text{g}}$	—	—	0.28	0.23
σ_{qe}	67.04	58.35	57.60	60.89
σ_{qsd}	—	—	4.92	2.04
σ_{tsd}	—	—	33.74	35.66
σ_{dd}	—	—	1.54	0.64
^{197}Au				
σ_{tot}	2976.26	2989.94	2859.84	2920.75
σ_{el}	1193.54	1206.10	1100.54	1150.99
σ_{sd}	—	—	32.55	11.95
$\sigma_{\text{sd}+\text{g}}$	—	—	0.29	0.24
σ_{qe}	62.94	54.69	61.15	64.53
σ_{qsd}	—	—	5.31	2.22
σ_{tsd}	—	—	35.82	37.80
σ_{dd}	—	—	1.66	0.69
^{208}Pb				
σ_{tot}	3052.11	3117.62	2955.57	3018.21
σ_{el}	1243.00	1274.60	1147.01	1199.14
σ_{sd}	—	—	32.88	12.02
$\sigma_{\text{sd}+\text{g}}$	—	—	0.29	0.24
σ_{qe}	62.55	54.11	61.01	64.39
σ_{qsd}	—	—	5.31	2.21
σ_{tsd}	—	—	35.73	37.71
σ_{dd}	—	—	1.66	0.69

TABLE II. RHIC.

	Glauber	Glauber + SRC	q -2 q model + SRC	3 q model + SRC
^{12}C				
σ_{tot}	413.71	425.73	406.90	410.20
σ_{el}	112.13	119.68	109.16	111.29
σ_{sd}	–	–	3.13	1.20
$\sigma_{\text{sd+g}}$	–	–	0.31	0.30
σ_{qe}	26.40	23.09	26.13	26.72
σ_{qsd}	–	–	0.95	0.29
σ_{tsd}	–	–	10.90	11.14
σ_{dd}	–	–	0.95	0.29
^{208}Pb				
σ_{tot}	3297.56	3337.57	3228.11	3262.58
σ_{el}	1368.36	1398.08	1314.04	1343.76
σ_{sd}	–	–	16.78	5.03
$\sigma_{\text{sd+g}}$	–	–	1.06	0.98
σ_{qe}	66.06	58.47	71.99	73.92
σ_{qsd}	–	–	2.39	0.56
σ_{tsd}	–	–	30.03	30.83
σ_{dd}	–	–	2.39	0.56

term, and diffractive gluon radiation, corresponding to the triple-Pomeron term ($IP\bar{P}P$). The former mostly contributes to small mass excitations, $d\sigma/dM_X^2 \propto 1/M_X^3$, whereas the latter is responsible for the large mass tail, $d\sigma/dM_X^2 \propto 1/M_X^2$, where M_X is the invariant mass of the produced system, $pp \rightarrow Xp$.

A. Coherent excitation of the projectile valence quark system

The cross section of coherent single diffraction on a nucleus, caused by excitation of the valence quark skeleton

TABLE III. LHC.

	Glauber	Glauber + SRC	q -2 q model + SRC	3 q model + SRC
^{12}C				
σ_{tot}	598.79	613.68	591.05	592.12
σ_{el}	198.11	208.59	194.84	195.65
σ_{sd}	–	–	0.74	0.20
$\sigma_{\text{sd+g}}$	–	–	2.58	2.56
σ_{qe}	49.10	45.42	45.03	45.22
σ_{qsd}	–	–	–0.66	–0.86
σ_{tsd}	–	–	6.97	7.00
σ_{dd}	–	–	–0.66	–0.86
^{208}Pb				
σ_{tot}	3850.63	3885.77	3833.26	3839.26
σ_{el}	1664.76	1690.48	1655.70	1660.67
σ_{sd}	–	–	2.62	0.59
$\sigma_{\text{sd+g}}$	–	–	2.58	2.56
σ_{qe}	120.92	112.65	113.37	113.88
σ_{qsd}	–	–	–2.08	–2.62
σ_{tsd}	–	–	17.55	17.63
σ_{dd}	–	–	–2.08	–2.62

without gluon radiation, is given as usual by the dispersion of the distribution of eigen elastic amplitudes, where the eigenstates are the dipoles [5,28]:

$$\sigma_{\text{sd}}(pA \rightarrow XA)_{IP\bar{P}P} = \int d^2b e^{I_A(b)} \left[\langle e^{-\sigma_{\text{dip}} T_A^h(b)} \rangle - \langle e^{-\frac{1}{2}\sigma_{\text{dip}} T_A^h(b)} \rangle^2 \right], \quad (57)$$

where $I_A(b)$ is given by Eq. (55). Dependent on the model, the dipole cross section here has the form of either Eq. (36) or Eq. (49), and the averaging is weighed by the wave function squared having the form of either Eq. (38) or Eq. (48).

Although Gribov corrections to the total cross section are known to be small, well within 10% [32,33], this is because they affect only the second exponential term in Eq. (8), which is small. However, this term itself is modified significantly by the inelastic shadowing corrections. Therefore one should expect a considerable increase of both terms in Eq. (57) owing to inelastic corrections, which make the nuclear medium considerably more transparent compared to the Glauber model [5]. Nevertheless, both terms are small for heavy nuclei and suppress diffraction everywhere, except at the nuclear periphery. Thus the cross section of single diffraction should rise as $A^{1/3}$, with a coefficient that is sensitive to the inelastic shadowing corrections and NN correlations.

The details of the calculations with both models under consideration can be found in Ref. [10]. The numerical results for several nuclei and energies are presented in Tables I, II, and III.

B. Coherent diffractive gluon radiation

Diffractive gluon radiation also contributes to the single-diffractive process $pA \rightarrow XA$. Correspondingly, the single-diffractive cross section [Eq. (57)] must be corrected for this excitation channel. The cross section of coherent gluon radiation on a nucleus is given by [19]

$$\begin{aligned} \sigma_{\text{sd}}(pA \rightarrow XA)_{3IP} &= \frac{3}{4\pi} \ln \left[\frac{s(1-x_0)}{M_0^2} \right] \int d^2b e^{I_A(b)} \langle e^{-\frac{1}{2}\sigma_{\text{dip}} T_A^h} \rangle^2 \\ &\times \int d^2r_T |\Psi_{qG}(\vec{r}_T)|^2 \left(1 - \exp \left\{ -\frac{9}{16} \left[\sigma_{\bar{q}q}(r_T, s) \right. \right. \right. \\ &\left. \left. \left. \times T_A^h(b) - \frac{9}{8} I_A(b) \right] \right\} \right)^2. \end{aligned} \quad (58)$$

Here $M_0^2 = 5 \text{ GeV}^2$ is the minimal effective mass squared of the proton excitation and $x_0 = 0.85$ is the minimal value of Feynman x , which can be treated as being in the domain of the triple-Regge kinematics [31].

The first factor in Eq. (58) accounts for the absorptive corrections, which arise from the lack of initial-final state interaction of the valence quarks propagating through the nucleus. Further details about the calculations can be found in Ref. [10]. The numerical results for several nuclei and energies are presented in Tables I, II, and III.

VI. QUASIELASTIC SCATTERING WITH AND WITHOUT EXCITATION OF THE PROJECTILE

In the cases when either the beam proton ($pA \rightarrow XA$) or the nucleus ($pA \rightarrow pA^*$) or both ($pA \rightarrow XA^*$) are diffractively excited, one can make use of completeness, which substantially simplifies the calculations. As was already mentioned, the important condition for the nucleus is that it decays into nuclear fragments with no new particle produced. The dipole formalism for these processes was developed in Ref. [10]. Here we rely on those results and introduce corrections related to NN correlations.

The simplest processes are double-excitation $pA \rightarrow XA^*$, where X includes the ground-state proton, as well as quasidiffraction, with all diffractive excitation of its valence quark system (without gluon radiation) and breakup of the nucleus. All channels of coherent interactions that leave the nucleus intact should be subtracted:

$$\begin{aligned} & \sigma_{\text{qel}}(pA \rightarrow pA^*) + \sigma_{\text{qsd}}(pA \rightarrow XA^*) \\ &= \int d^2b \langle e^{-\sigma_{\text{dip}} T_A^h(b)} \{ e^{\tilde{I}_A(b)} e^{\frac{\sigma_{\text{dip}}^2 T_A^h(b)}{16\pi B_{\text{el}}}} - e^{I_A(b)} \} \rangle \\ &= \int d^2b \sum_{k=0} \frac{1}{k!} \left[\frac{T_A^h(b)}{16\pi B_{\text{el}}} \right]^k [e^{\tilde{I}_A(b)} - e^{I_A(b)} \delta_{k0}] \\ &\quad \times \frac{\partial^{2k}}{\partial (T_A^h)^{2k}} \langle e^{-\sigma_{\text{dip}} T_A^h(b)} \rangle. \end{aligned} \quad (59)$$

Here, besides the function $I_A(b)$ defined in Eq. (55), we introduce a new one:

$$\begin{aligned} & \tilde{I}_A(b) \\ &= \int d^2l_1 d^2l_2 \Delta_A^\perp(\vec{l}_1, \vec{l}_2) [2\text{Re} \Gamma^{\bar{q}q}(\vec{l}_1, \vec{r}_T, \alpha) \\ &\quad - (\text{Re} \Gamma^{\bar{q}q}(\vec{l}_1, \vec{r}_T, \alpha))^2] [2\text{Re} \Gamma^{\bar{q}q}(\vec{l}_2, \vec{r}_T, \alpha) \\ &\quad - (\text{Re} \Gamma^{\bar{q}q}(\vec{l}_2, \vec{r}_T, \alpha))^2] \approx \left[\frac{\sigma_{\text{tot}}^{pN} - \sigma_{\text{el}}^{pN} - \sigma_{\text{sd}}^{pN}}{\sigma_{\text{tot}}^{pN}} \right]^2 I_A(b). \end{aligned} \quad (60)$$

To simplify the calculations, we neglect here the difference in the slopes of powers of the partial amplitude. This is a second-order correction, that is, a correction to a correction.

One can single out in Eq. (59) the quasielastic channel. For that purpose, one should average over the dipole sizes separately for both the incoming and outgoing protons:

$$\begin{aligned} \sigma_{\text{qel}}^{pA} &= \int d^2b \langle \left(e^{-\frac{1}{2}\sigma_{\text{dip}}^{(1)} T_A^h(b)} e^{-\frac{1}{2}\sigma_{\text{dip}}^{(2)} T_A^h(b)} \right. \\ &\quad \left. \times \left[e^{\tilde{I}_A(b)} e^{\frac{1}{16\pi B_{\text{el}}} \sigma_{\text{dip}}^{(1)} \sigma_{\text{dip}}^{(2)} T_A^h(b)} - e^{I_A(b)} \right] \right) \rangle_2 \\ &= \int d^2b \sum_{k=0} \frac{1}{k!} \left[\frac{T_A^h(b)}{4\pi B_{\text{el}}} \right]^k [e^{\tilde{I}_A(b)} - e^{I_A(b)} \delta_{k0}] \\ &\quad \times \left\{ \frac{\partial^k}{\partial (T_A^h)^k} \langle e^{-\frac{1}{2}\sigma_{\text{dip}} T_A^h(b)} \rangle \right\}^2. \end{aligned} \quad (61)$$

This is a fast-converging series because of the smallness of the elastic cross section. We control the accuracy to be within 1%.

Subtracting Eq. (61) from Eq. (59), one can get the quasidiffractive cross section, which includes the proton excitations without gluon radiation. To include gluon radiation, we use the same prescription as in Eq. (54), replacing the $IP\bar{I}P\bar{I}R$ term, $[\sigma_{\text{sd}}^{pp}]_{IP\bar{I}P\bar{I}R}$, by the total single-diffraction cross section.

In the case of nuclear breakup, the recoil-bound nucleon can also be diffractively excited. We relate the cross sections for such channels to the previously calculated quasielastic and quasidiffractive processes, in the same way as in Ref. [10].

VII. GLUON SHADOWING

In terms of the parton model, gluon shadowing is interpreted in the nuclear infinite momentum frame as a result of fusion of gluons originating from different bound nucleons. This process leads to a reduction of the gluon density in the nucleus at small x . The ultimate form of gluon shadowing is gluon saturation [34].

In terms of the dipole approach, gluon shadowing is described as Glauber shadowing for higher Fock states containing gluons [19]. The effect turns out to be rather weak because of the shortness of the quark-gluon and gluon-gluon correlation radius, an observation that is supported by much experimental evidence [35,36]. For this reason, we neglect the small effects of nucleon correlations in the calculation of gluon shadowing and use the results of Ref. [10].

VIII. CONCLUSIONS

In this article, we further developed the dipole approach of Refs. [5,9,10] to the calculation of Gribov inelastic corrections. We employed two models for the proton wave function, which result in reasonable diffractive cross sections for pp collisions. Here we increased the accuracy of the calculation of the cross sections of different diffractive processes on nuclei by improving the model for the nuclear wave function. Namely, we went beyond the popular single-particle density approximation and introduced corrections for nucleon-nucleon correlations, which lead to sizable effects, modifying the effective nuclear thickness function [12]. While inelastic shadowing corrections make the nuclear medium more transparent for colorless hadrons, the nucleon short-range correlations work in the opposite direction, making the medium more opaque. The influence of both effects on different diffractive channels varies. Effects are especially large for quasielastic and quasi-single-diffractive processes associated with the survival probability of colorless hadrons propagating through a nuclear medium. Notice that for heavy nuclei, the effect of correlations is sometimes smaller than the uncertainty brought by poor knowledge of the proton structure. This allows us to gain new information about the proton wave function, provided that precise data for nuclear cross sections will be available.

ACKNOWLEDGMENTS

This work was supported in part by Fondecyt, Chile (Grant Nos. 1090236 and 1090291) and by DFG, Germany (Grant No. PI182/3-1). C.D.A. thanks the HELEN project for support during his visit to the Department of Physics, UTFSM, Valparaiso, where this work was initiated. M.A. was supported

by a DOE grant under Contract No. DE-FG02-93ER40771; he also thanks HPC-EUROPA2 (Project No. 228398) with the support of the EU Research Infrastructure Action FP7. This work was finished during an extended visit by the authors to INT, University of Washington; they are thankful to the INT staff for support and warm hospitality.

-
- [1] R. J. Glauber, in *Lectures in Theoretical Physics*, edited by W. E. Brittin *et al.* (Interscience Publisher's Inc., New York, 1959).
- [2] V. N. Gribov, *Sov. JETP* **29**, 483 (1969); J. Pumplin and M. Ross, *Phys. Rev. Lett.* **21**, 1778 (1968).
- [3] V. Karmanov and L. A. Kondratyuk, *Sov. Phys. JETP Lett.* **18**, 266 (1973).
- [4] B. Z. Kopeliovich and L. I. Lapidus, *Pisma Zh. Eksp. Teor. Fiz.* **28**, 664 (1978).
- [5] B. Z. Kopeliovich, L. I. Lapidus, and A. B. Zamolodchikov, *JETP Lett.* **33**, 595 (1981) [*Pisma Zh. Eksp. Teor. Fiz.* **33**, 612 (1981)].
- [6] B. Z. Kopeliovich, J. Raufeisen, and A. V. Tarasov, *Phys. Lett.* **B440**, 151 (1998).
- [7] B. Z. Kopeliovich, J. Raufeisen, and A. V. Tarasov, *Phys. Rev. C* **62**, 035204 (2000).
- [8] B. Z. Kopeliovich, I. Schmidt, and M. Siddikov, *Phys. Rev. D* **80**, 054005 (2009).
- [9] B. Z. Kopeliovich, *Phys. Rev. C* **68**, 044906 (2003).
- [10] B. Z. Kopeliovich, I. K. Potashnikova, and I. Schmidt, *Phys. Rev. C* **73**, 034901 (2006).
- [11] R. Subedi *et al.*, *Science* **320**, 1476 (2008); E. Piasetzky, M. Sargsian, L. Frankfurt, M. Strikman, and J. W. Watson, *Phys. Rev. Lett.* **97**, 162504 (2006); A. Tang *et al.*, *ibid.* **90**, 042301 (2003); R. Shneor *et al.*, *ibid.* **99**, 072501 (2007).
- [12] M. Alvioli, C. Ciofi degli Atti, I. Marchino, V. Palli, and H. Morita, *Phys. Rev. C* **78**, 031601(R) (2008).
- [13] L. L. Foldy and J. D. Walecka, *Ann. Phys.* **54**, 447 (1969).
- [14] M. Alvioli, C. Ciofi degli Atti, H. Morita, and V. Palli (to be unpublished).
- [15] M. Alvioli, C. Ciofi degli Atti, and H. Morita, *Phys. Rev. C* **72**, 054310 (2005).
- [16] M. Alvioli, C. Ciofi degli Atti, and H. Morita, *Phys. Rev. Lett.* **100**, 162503 (2008).
- [17] B. S. Pudliner, V. R. Pandharipande, J. Carlson, S. C. Pieper, and R. B. Wiringa, *Phys. Rev. C* **56**, 1720 (1997).
- [18] H. De Vries, C. W. De Jager, and C. De Vries, *Nucl. Data Tables* **36**, 495 (1987).
- [19] B. Z. Kopeliovich, A. Schäfer, and A. V. Tarasov, *Phys. Rev. D* **62**, 054022 (2000).
- [20] S. Amendolia *et al.*, *Nucl. Phys.* **B277**, 186 (1986).
- [21] I. A. Schmidt and R. Blankenbecler, *Phys. Rev. D* **15**, 3321 (1977).
- [22] M. Anselmino, E. Predazzi, S. Ekelin, S. Fredriksson, and D. B. Lichtenberg, *Rev. Mod. Phys.* **65**, 1199 (1993).
- [23] B. Z. Kopeliovich and B. G. Zakharov, *Phys. Lett.* **B211**, 221 (1988); *Sov. J. Nucl. Phys.* **48**, 136 (1988); **49**, 674 (1989); *Z. Phys. C* **43**, 241 (1989); *Sov. Phys. Part. Nucl.* **22**, 140 (1991).
- [24] B. Z. Kopeliovich, H. J. Pirner, A. H. Rezaeian, and I. Schmidt, *Phys. Rev. D* **77**, 034011 (2008).
- [25] B. Z. Kopeliovich, I. K. Potashnikova, I. Schmidt, and J. Soffer, *Phys. Rev. D* **78**, 014031 (2008).
- [26] B. Z. Kopeliovich, A. H. Rezaeian, and I. Schmidt, *Phys. Rev. D* **78**, 114009 (2008).
- [27] Y. V. Kovchegov, *Phys. Rev. D* **64**, 114016 (2001); **68**, 039901(E) (2003).
- [28] B. Z. Kopeliovich, I. K. Potashnikova, and I. Schmidt, *Braz. J. Phys.* **37**, 473 (2007).
- [29] Y. P. Ivanov, B. Z. Kopeliovich, A. V. Tarasov, and J. Hufner, *Phys. Rev. C* **66**, 024903 (2002).
- [30] B. Z. Kopeliovich, J. Nemchik, A. Schaefer, and A. V. Tarasov, *Phys. Rev. C* **65**, 035201 (2002).
- [31] Y. M. Kazarinov, B. Z. Kopeliovich, L. I. Lapidus, and I. K. Potashnikova, *JETP* **70**, 1152 (1976).
- [32] P. V. R. Murthy *et al.*, *Nucl. Phys.* **B92**, 269 (1975).
- [33] A. Gsponer *et al.*, *Phys. Rev. Lett.* **42**, 9 (1979).
- [34] L. V. Gribov, E. M. Levin, and M. G. Ryskin, *Nucl. Phys.* **B188**, 555 (1981); *Phys. Rep.* **100**, 1 (1983).
- [35] B. Z. Kopeliovich and B. Povh, *J. Phys. G* **30**, S999 (2004).
- [36] B. Z. Kopeliovich, I. K. Potashnikova, B. Povh, and I. Schmidt, *Phys. Rev. D* **76**, 094020 (2007).